

**Summer Research Project 2008**  
**Photocell Detection System and Self-Supporting**  
**Aluminum Target Preparation**

Michael Carilli  
Chris Schmitt  
Advisor Philippe Collon  
University of Notre Dame

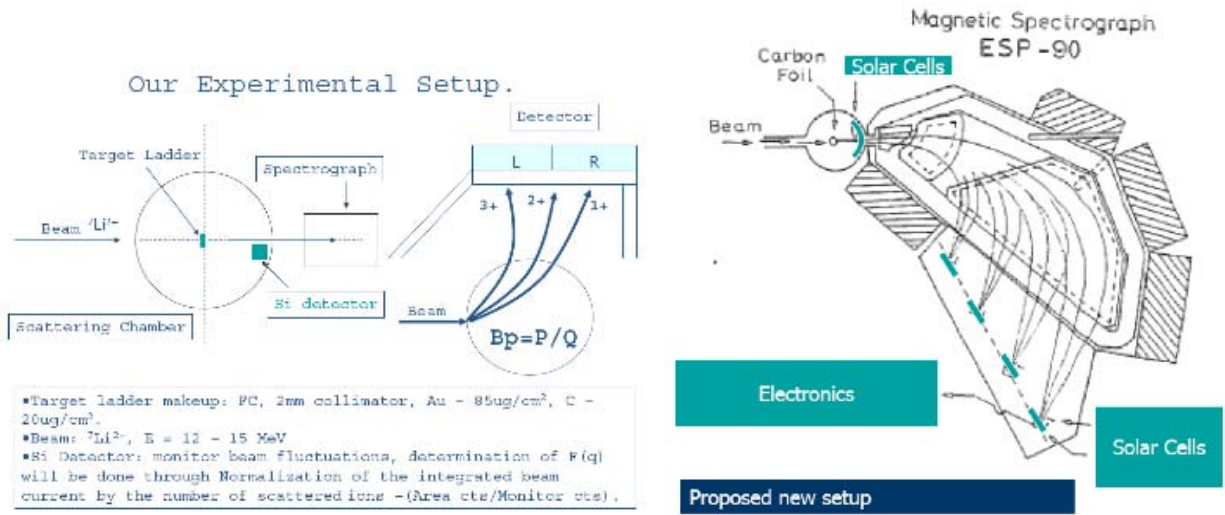


Figure 1.1: Left: The charge state distribution measurement system in its current setup. Right: The proposed new system.

# Abstract

This paper presents a summary of a summer undergraduate research project conducted under Chris Schmitt and Dr. Philippe Collon with the assistance of a grant from the University of Notre Dame’s College of Science. First, it describes work towards implementing a new charge state distribution detector system for the 10 MeV tandem accelerator. This system will use photocells instead of expensive, delicate silicon detectors. Second, it discusses the preparation of self-supporting foil targets for accelerator beam, intended to be used in conjunction with the new detector system.

## 1 Photocell Detectors

### 1.1 Current System

Figure 1.1 depicts the detector system currently in place for measuring the charge state distribution of a beam of atoms (in this case lithium) after passing through a thin foil. A particle counter is placed along the projected path of each resulting charge state.

In its current configuration, the 10 MeV accelerator uses silicon detectors as particle counters. Although these devices provide very fine energy resolution, they are quite delicate and costly. Such high resolution is superfluous since all the detector system needs is a means of counting particles, not a precise measurement of their energies. Therefore it is proposed that the silicon detectors be replaced with more simple photocells. These photocells are sturdier and significantly cheaper, costing on the order of \$20 apiece.

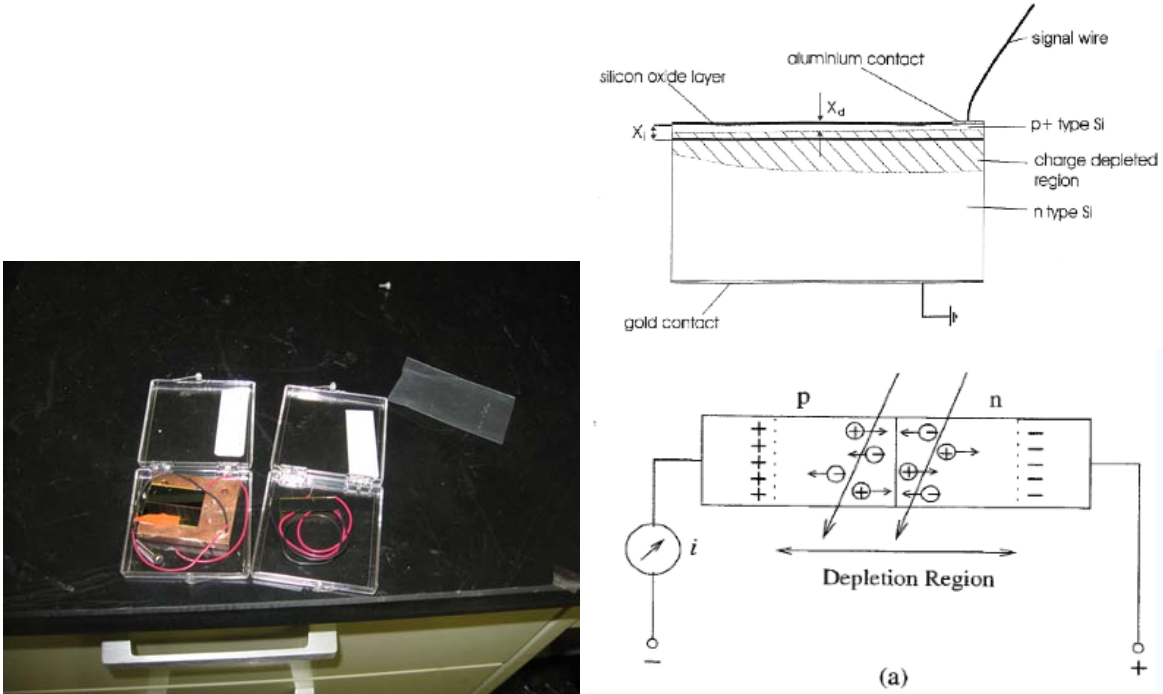


Figure 1.2: Left: A picture of the photocells. Right: A schematic demonstrating how semiconductor photocells work (from Chris Schmitt, 2008).

### 1.2 Background

Photocell detectors are, in essence, a sandwich of two types of semiconductor material (in our case silicon). Half consists of a “P-type” semiconductor doped with boron or some other Group III element; the other half is made of an “N-type” semiconductor doped with arsenic or some other Group V element. Both are conductive, albeit in opposite ways: In P-type semiconductors the electrons are stationary but holes (absences of electrons) are mobile, while in N-type semiconductors the electrons are mobile and the holes are stationary. When negative voltage bias is applied to the P side, positively charged holes are drawn away from the interface between the two materials. Similarly, electrons on the N side are repelled from the interface. This creates a non-conductive depleted region along the interface that is free of mobile charge carriers. However, anything impacting the depleted region (radiation, for instance, will knock loose some electrons, creating electron-hole pairs. Since the depleted region has a voltage across it, the electron and its corresponding hole immediately move off in opposite directions, creating a current that can be measured (Schmitt, 2008). The energy of the incident radiation can be estimated as well: More energetic impacts will knock more electrons free and create higher current magnitudes.

A small amount of leakage current across the depleted region is unavoidable. The leakage current is

roughly proportional to the applied negative bias up until a certain point. If it gets too high, moving electrons will begin to create electron-hole pairs of their own just like incident radiation might; these newly released electrons will begin moving and perhaps create electron-hole pairs in turn, in a sort of cascade effect. The leakage current will begin to climb much more rapidly. Ideally, one wants to find the negative bias at which the photocell performs best without causing this breakdown.

### 1.3 Optimization

To find the ideal voltage for our photocells, we placed them near an  $\alpha$  emitter ( $^{241}\text{Am}$ ) under vacuum. We found that ideal performance (as indicated by superior energy resolution) was achieved with a negative bias of around 10 V. Breakdown seemed to occur in the neighborhood of -13 V (see figure 1.3 for both data sets).

Unfortunately, roughly half of the photocells we bought were defective, undergoing breakdown at around -6 V and exhibiting leakage currents that started roughly twice as high as normal values and increased steadily with time. We tested all photocells for abnormal breakdown behavior to determine which ones might work for the new detection system.

We also placed some photocells directly in the path of the accelerator beam for various periods of time, to assess the effects of heavy or prolonged radiation exposure. Irradiated cells tended to have significantly lower energy resolution and significantly higher leakage currents.

Finally, we tested the cells' counting efficiency by placing them a fixed distance from a  $^{241}\text{Am}$  source of known activity and comparing their measured rates of  $\alpha$  particle emission to expected theoretical rates. The good cells never performed worse than 80% and often achieved efficiencies as high as 98%, indicating that they are suitable for use in our new detection system.

## 2 Target Preparation

### 2.1 Goals

At the beginning of the summer, three goals were proposed with respect to target preparation: 1. that we compile a database containing as much literature as possible on the subject of self-supporting targets, 2. that we use this information to prepare self-supporting targets of carbon, aluminum, gold, silver, copper, chromium, titanium, iron, nickel, zinc, tin, and manganese, adding our own experiences in making these targets to the database for future reference, and 3. that we then use these foils in the accelerator to build

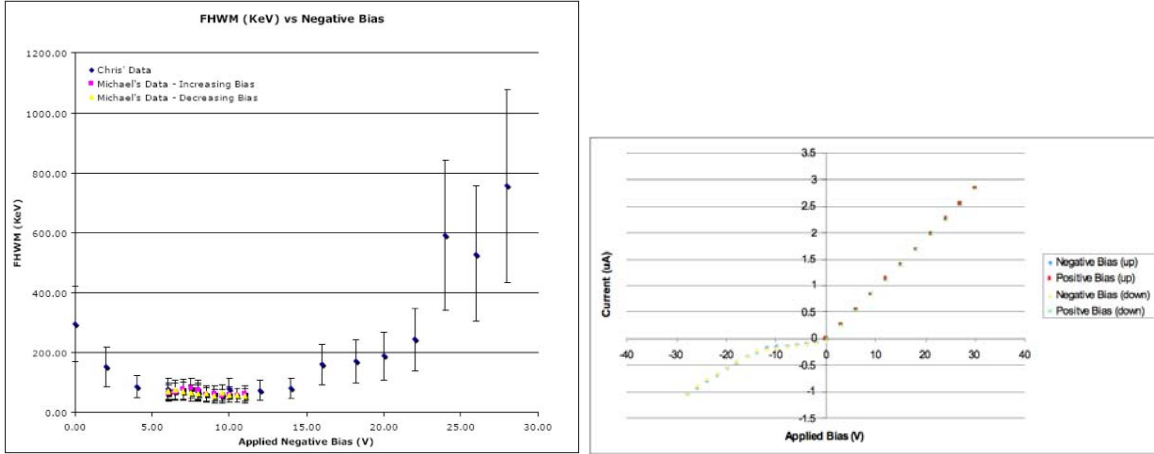


Figure 1.3: Left: Energy resolution vs. applied negative bias behavior for a typical (good) cell. Right: Leakage current versus applied negative bias.

on the results of a paper by Itoh et al (1999) on the charge state distribution resulting when a lithium beam is passed through a carbon foil.

Gold targets and carbon targets proved fairly straightforward to produce; however, aluminum was much more difficult to work with and required a great deal of trial and error. It ended up taking all summer to find a reliable means of producing self-supported aluminum targets.

## 2.2 The Process—Overview

The desired end result of the self-supporting target preparation process is a thin, uniform, free-standing film or foil of target material mounted in such a way that a properly collimated accelerator beam can easily be passed through it without obstruction or interference from anything but the foil itself. Current literature outlines many methods for producing these targets, such as rolling (if the target material is sufficiently malleable), cracking (useful for carbon), electrodeposition, and vacuum evaporation.

We dealt exclusively with the last of these techniques. The general method for producing self-supporting targets by evaporation, as outlined by Maxman, Muggleton and many others, runs as follows:

First, a borosilicate glass slide is coated with some sort of water-soluble release agent. Commonly used release agents include Teepol (a detergent), barium chloride, sucrose, and betaine. Next, a sample of the desired target material (ie. gold, aluminum, etc) is placed in a boat or crucible. The material is then placed beneath the slide under high vacuum, and heated until a thin layer has evaporated out of the boat or crucible onto the slide. The slide is then slowly lowered into a hot-water bath at approximately a 45 degree angle with the thin layer side up. If everything has been done properly, the release agent will dissolve, causing the

layer of evaporated material to float off onto the surface of the water in the form of a thin foil. This foil is then (very carefully, because it is invariably quite delicate) scooped from the surface of the water onto some sort of target mount.

### 2.3 Our Evaporator

Our evaporator consists of a bell jar in which vacuum is maintained using a diffusion pump backed by a mechanical pump. This system is capable of consistently achieving a vacuum pressure of  $8.0 \times 10^{-6}$  torr.

Target material is placed in a tungsten, tantalum, or molybdenum boat, which is then attached across a pair of externally controlled current leads. Current is passed through the boat, and resistive heating causes the material to evaporate.

Once evaporation is complete, the bell jar is vented with argon gas, to avoid any potential reactions that might occur between air and the still-cooling target material.

### 2.4 Thickness Measurement

In any self-supporting target preparation process it is essential to know the thickness of the targets one is producing. For evaporation, the standard way to do this is to place quartz crystal monitors (see figure 2.1) in vacuum next to the glass slide or substrate. As material evaporates onto the substrate, some of it (an approximately equal amount, if the monitor and the substrate are sufficiently close) will be deposited onto the crystal monitor, changing its resonant frequency. This change in resonant frequency can be measured, and is directly proportional to the thickness of the deposited material in  $\mu\text{g}/\text{cm}^2$ :

$$df_0 = -\frac{f_0^2}{NP_q} \frac{dm}{A} \quad (2.1)$$

where  $P_q$  is the density of quartz,  $N$  is a frequency constant (1670 kHz/mm for AT-cut crystals, and  $\frac{dm}{A}$  is the deposited mass per unit area (Behrdnt and Love, 1962). A more complete description of the use of quartz crystal oscillators can be found in that article, or in Muggleton and Howe (1964).

Crystal monitors merely provide the experimenter with a degree of knowledge and control during the actual evaporation process. It is also important to measure the thickness by other means once evaporation is complete.

One way this can be done is by using a sensitive balance to find the mass of the substrate material (in our case the slide) before and after evaporation. The difference between those two measurements is the mass



Figure 2.1: One of the two quartz crystal monitors used in our evaporator.

of material that has been evaporated onto the substrate; all one must do is divide by the deposition area to obtain the thickness. A similar procedure was outlined by Maxman (1966). We attempted to use this technique as well; however, our balance turned out to be insufficiently precise.

Another way to measure the thickness of finished foils is to pass a stream of particles through them and measure the energy loss. After the entire target-making process is complete and the foils have already been floated and placed in their target mounts, each one is taken in turn and placed between a silicon detector and an  $\alpha$ -emitter such as  $^{241}\text{Am}$  under vacuum. We then use the silicon detector and a program called Maestro to measure the resulting energy distribution. Since the energy distribution of  $\alpha$ -particles emerging from an unshielded  $^{241}\text{Am}$  source is well known (see figure 2.2), we can record the energy difference  $\Delta E$  between the observed main peak and the expected main peak for an unaltered  $^{241}\text{Am}$  source. We then use a program called SRIM to estimate the expected energy loss per unit thickness. For  $\alpha$ -particles in aluminum, this value is  $0.5698 \text{ KeV}/(\mu\text{g}/\text{cm}^2)$ . The thickness  $T$  is then given by

$$T = \frac{\Delta E}{0.5698} \quad (2.2)$$

## 2.5 Aluminum

We set out to prepare targets of four separate thicknesses: 5, 10, 20, and  $40 \mu\text{g}/\text{cm}^2$ , corresponding to frequency changes of 407, 814, and 1628, and 3256 Hz respectively. Muggleton's review of target-making procedures states that making self-supported aluminum targets is a fairly straightforward process; the standard technique of coating a slide with Teepol and floating should work. We consulted John Greene at

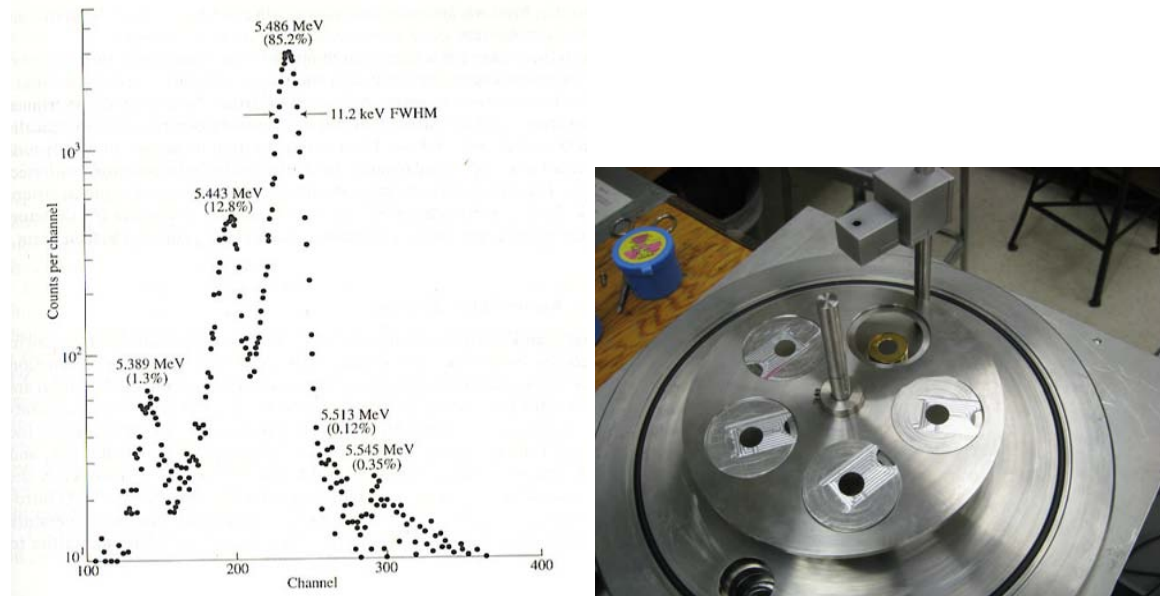


Figure 2.2: Left: The energy distribution of  $\alpha$ -particles emitted by  $^{241}\text{Am}$ . Right: The thickness measurement apparatus.

Argonne National Laboratories on how to properly prepare the slides: Apply a thin layer of teepol, let it dry, then wipe it away until the layer is no longer visible.

We tried this at first, but could not get the foils to float free from the slides after evaporation. If we left a thick layer of teepol on the slides the foils would float, but irregularities in the teepol surface caused them to be fragmented, warped and unusable. Treating the slides with solutions of teepol and water at various concentrations proved equally ineffective at getting the foils to float properly.

Next, we tried using sodium chloride as a release agent. Barium chloride is the release agent most authors suggest; however, it is toxic and we wanted to be sure normal salt was not equally serviceable before risking the use of  $\text{BaCl}_2$ . We evaporated a salt layer, then evaporated aluminum on top of that. Instead of forming an aluminum foil on the sodium chloride, the aluminum created a smoky film that dissolved away completely when we attempted to float it.

Up until this point we had been evaporating with the slides a relatively short distance ( 10 cm) above the boat to speed the evaporation process. We hypothesized that this short distance between the heated material and the substrate might be causing heat ablation of release agents. Teepol has a low melting point, somewhere between 100 and 200  $^\circ\text{C}$  (Maxman). Therefore, we decided to run subsequent evaporations with the slides about 24 cm above the boat. Another benefit of that approach is that it increased deposition uniformity across the slides. Material evaporated from a point source has an angular distribution proportional to  $\cos^2\theta$ ,

where  $\theta$  is the angle from the vertical (Greene, 2004). By increasing their distance from the evaporation source, we reduced the angle the slides subtended across this distribution.

We also began using new slides. The old ones were becoming too rough with repeated use and cleaning.

This new configuration proved a good deal more successful. We retraced all of our previous release agent application techniques, and added a new detergent (Dawn dishwashing soap) to the rotation. With Dawn, we produced several usable targets. The most effective release agent proved to be Teepol, applied thickly and allowed to dry for a day, then rubbed off with circular strokes using KimWipes or some other sterile tissue until almost clear. It is unknown why circular strokes worked better than straight strokes for producing viable slides.

During the actual floating process, we found it most effective to use deionized water heated to a temperature of approximately 80 °C. Scraping the edges of the slides with a razor blade prior to floating also made the foils release more smoothly. The razor blade was also used to divide each deposited film into 4 chunks (as seen in figure 2.3), so that 4 targets could potentially be produced from each slide. When lifting the floating foils from the surface of the water onto the target mount, we found it most effective to lift at a nearly vertical angle, since small water droplets clinging to the foil would otherwise create a transverse force that tended to break the foil. Maxman recommends adding a few drops of Teepol to the surface of the water to minimize surface tension stress on the foil during the lifting process; we followed his advice and found it to be helpful.

Figure 2.4 gives a summary of the various slide coating techniques, together with approximately how successful each one was at producing viable aluminum targets.

It should also be noted that all three boat types (tantalum, molybdenum, and tungsten) were tried. Boats made of all three materials alloyed with the aluminum and had to be discarded eventually, but of the three, tungsten proved the most consistent and least prone to alloying.

No positive results were achieved for thicknesses less than  $\Delta f = 814$  Hz, however.

### 3 Conclusion

Unforeseen setbacks caused us to fall short of the goals we intended to accomplish this summer. However, we are now prepared to proceed with implementing the photocell detection system. We have also found a proven, reliable means of producing aluminum targets. Hopefully, this target-making technique will prove equally effective for other materials, and future research will not need to suffer the same difficulties.



Figure 2.3: The target making process from beginning to end. In order from left to right and top to bottom: 1: The evaporator interior. 2: Slides newly coated with aluminum. 3: Properly scraped slides ready for floating. 4: Floating. 5: Mounting on the target holder. 6: The finished product (aluminum, gold, and carbon shown)

<b>Treatment Method:</b>	<b>Distance between slide and material</b>	<b>Results</b>	<b>Overall Success Rate</b>
Teepol, dried on and wiped clear	10 cm	$\Delta f = 814$ : Foil did not release.	0%
		$\Delta f = 1624$ : Foil did not release.	0%
Teepol, dried on and wiped smooth but thick	10 cm	$\Delta f = 814$ : Foil released but fragmented.	0%
		$\Delta f = 1624$ : Foil released but fragmented.	10%
Sodium chloride	10 cm	$\Delta f = 814$ : Foil formed smoky soluble film.	0%
		$\Delta f = 1624$ : Foil formed smoky soluble film.	0%
Sodium chloride	24 cm	$\Delta f = 814$ : Foil formed smoky soluble film.	0%
		$\Delta f = 1624$ : Foil formed smoky soluble film.	0%
Dawn, dried on and wiped clear	24 cm	$\Delta f = 814$ : Foil releases, but inconsistently.	25%
		$\Delta f = 1624$ : Foil releases but inconsistently.	25%
Dawn, dried on and wiped smooth but thick	24 cm	$\Delta f = 814$ : Foil releases but is poor quality; often breaks.	25%
		$\Delta f = 1624$ : Foil releases but is poor quality.	50%
Teepol, dried on and wiped clear with straight strokes	24 cm	$\Delta f = 814$ : Releases in bits, inconsistently.	10%
		$\Delta f = 1624$ : Releases in bits, inconsistently.	10%
Teepol, dried on and wiped clear with circular strokes	24 cm	$\Delta f = 814$ : Releases slowly but smoothly and nicely.	75%
		$\Delta f = 1624$ : Releases slowly but smoothly and nicely.	75%

Figure 2.4: Summary of results for various slide treatment and placement methods.

## References

- [1] Adair, H. "Target Thickness and Uniformity Measurements Using Charged Particles." *Nuclear Instruments and Methods* 102 (1979), pgs. 599-610.
- [2] Behrndt, K., and R. Love. "Automatic Control of Film-Deposition Rate with the Crystal Oscillator for Preparation of Alloy Films." *Vacuum*, 1962, pgs. 1-10.
- [3] Greene, John. Private communication, 4/21/08.
- [4] Greene, John. "The Alchemy of Target Making." Notre Dame Physics Department Colloquium. Newland Science Hall, University of Notre Dame, Notre Dame, IN. 8/4/2004.
- [5] Holland, L. *Vacuum Deposition of Thin Films*. London: Chapman and Hall, 1956.
- [6] Itoh, A., H. Tsuchida et al. "Equilibrium charge distributions of lithium ions emerging from a carbon foil." *Nuclear Instruments and Methods in Physics Research B* 159 (1999), pgs. 22-27
- [7] Maxman, S. "Target Preparation Techniques." *Nuclear Instruments and Methods* 50 (1967), pgs. 53-60.
- [8] Muggleton, A. "Preparation of thin nuclear targets." *Journal of Physics E* 12 (1979), pgs 780-807.
- [9] Muggleton, A. "Deposition techniques for the preparation of thin film nuclear targets." *Vacuum* 37 (1987), pgs. 785-817.
- [10] Muggleton, A., and F. Howe. "Crystal Oscillator Film Thickness Monitor." *Nuclear Instruments and Methods* 28 (1964), pgs. 242-244.
- [11] Schmitt, C. "2008 Project Review." Unpublished internal Notre Dame Physics Department communication, 2008.